Interfacial charge transfer in blue organic light-emitting diode with extremely low turn-on voltage

Seiichiro Izawa, Materials and Structures Laboratory, Institute of Integrated Research, Institute of Science Tokyo

Abstract

Organic light-emitting diodes (OLEDs) are already commercially available and used in smartphones and large-screen televisions because they can display vivid images. However, blue OLEDs typically require high driving voltages due to the high energy of blue light, which often limits device stability and power efficiency. To address this issue, blue upconversion (UC)-OLEDs that utilize triplet-triplet annihilation (TTA) to achieve emission at an ultra-low voltage of approximately 1.5 V have been developed. This study investigates the fundamental single-electron transfer process from the interfacial charge-transfer (CT) state to the triplet excited state (T_1) of the blue TTA emitter molecule, which is relevant to the emission process of blue UC-OLED. Firstly, the CT state and T_1 energies of 45 different combinations of anthracene-based donors and naphthalene diimide-based acceptors were estimated by the optical methods. As a result, a correlation between the energy difference (between the CT state and T_1) and TTA-UC emission efficiency that is mainly governed by the single electron transfer process between these states is discussed based on Marcus theory. The results demonstrate that the transfer process is most efficient when the energy difference is near zero. This finding indicates that facilitating efficient transitions and minimizing voltage loss could be realized at the same time. These insights offer a strategic framework for optimizing low-voltage blue OLEDs for future energy-saving display and lighting technologies

Keywords: Organic light-emitting diode, Organic semiconductor interface, Upconversion, Charge transfer state, Triplet excited state, Energy transfer

1. Introduction

Organic light-emitting diodes (OLEDs) are already commercially available and used in smartphones and large-screen televisions because they can display vivid images. Furthermore, in recent years, their applications have expanded to include projectors for VR headsets, PC monitors, and in-vehicle displays. The power consumption of OLEDs is expressed by the formula: current × voltage = power. First, regarding current efficiency, it has been optimized through the development of phosphorescent molecules that can emit light from the triplet excited state (T_1)—which is generally dark state but is generated at a rate of 75%—via the heavy-atom effect[1], as well as thermally activated delayed fluorescence (TADF) molecules capable of converting T_1 into the luminescent singlet excited state (S_1)[2], and there have been reported to achieve 100% internal efficiency in converting current to light. On the other hand, the driving voltage for OLED devices remains high. In particular, among the three primary colors of light—red, green, and blue—blue light emission at approximately 460 nm, which has the highest light energy, requires a driving voltage of about 4 V to achieve the luminance level of a smartphone display[3]. Furthermore, the high energy of blue light leads to a reduction in device lifetime. While devices using high-efficiency phosphorescent molecules have been commercialized for red and green pixels, traditional fluorescent molecules such as anthracene derivatives are still used for blue pixels. This is because the energy of blue light is comparable to the carbon-nitrogen bond energy of organic molecules; consequently, blue phosphorescent molecules and TADF molecules (Figure 1), which can form high-energy, long-lived T_1, are prone to molecular decomposition, making it difficult in principle to improve their stability[4]. On the other hand, anthracene derivatives, which are fluorescent molecules, have a low T_1 level and are stable, making them highly valued in commercial devices. However, since light can be mainly generated from the S_1 level, which accounts for approximately 25% of the generated states, the luminous efficiency is low. Furthermore, a voltage greater than the molecular bandgap energy must be applied, resulting in a high drive voltage (Figure 1).

In recent years, we have developed a blue upconversion (UC)-OLED driven by ultra-low voltage that can selectively excite the low-energy T_1 state of anthracene derivatives via a charge transfer (CT) state generated at the interface with naphthalene imide derivatives, and subsequently generate a high-energy S_1 through a triplet-triplet annihilation (TTA) UC process to produce light (Figure 1)[5, 6, 7]. Anthracene derivatives have an energy of approximately 1.7 eV for T_1 and approximately 2.9 eV for S_1. Since they satisfy the energy relationship $2T_1 > S_1$, they have been widely used as TTA emitters for photon upconversion. When compared to the driving principle of conventional OLEDs, unlike fluorescent OLEDs where S_1 and T_1 are generated in a ratio of 25% to 75% through

electrical excitation, UC-OLEDs are characterized by the selective excitation of only the low-energy T_1 state by utilizing the CT state at the interface as a precursor, even though the same anthracene derivatives are used (Figure 1). As a result, we succeeded in emitting blue light of approximately 3 eV at an ultra-low voltage of about 1.5 V, which is impossible with conventional OLED (Figure 2a). Here, the most critical transition process leading to light emission in UC-OLED is the transition from the CT state generated at the donor/acceptor (D/A) interface—composed of an anthracene derivative and a naphthalene diimide derivative—to the generation of T_1 in the anthracene derivative. From a microscopic perspective, this is a process in which a single electron transfers from the naphthalene imide derivative to the anthracene derivative at the solid-state interface (Figure 2b). Since such single-electron transfer processes at solid-state interfaces are common in various devices, such as OLEDs and organic solar cells, elucidating their behavior is important not only for improving the efficiency of UC-OLEDs but also for clarifying the fundamental processes underlying organic devices. A characteristic of UC-OLEDs is that the emission from the CT state and the S_1 emission following TTA-UC appear at significantly different wavelengths. Therefore, by observing the intensity of TTA-UC emission, it is possible to discuss the formation efficiency of T_1, which is dark state and normally difficult to observe; furthermore, since the energies of these levels can be estimated from the wavelengths of CT emission and T_1 phosphorescence, UC-OLEDs are a suitable system for detailed observation of the transition processes between excited states at these interfaces.

In this study, we fabricated a total of 45 devices with different energy levels at the D/A interface by combining three types of anthracene derivative donor molecules with 15 types of naphthalene imide derivative acceptor molecules, and observed the TTA-UC emission intensity of each device. Furthermore, by observing CT emission at the D/A interface and T_1 emission from anthracene derivatives, we conducted research aimed at clarifying the effect of the energy difference between these states on the single electron transfer process accompanying the transition from the CT state to the T_1 state[8].

2. Single-Electron Transfer Processes Using Marcus Theory

Electron transfer processes are fundamental processes that govern chemical and biological reactions, and their rates are primarily discussed using Marcus theory, which

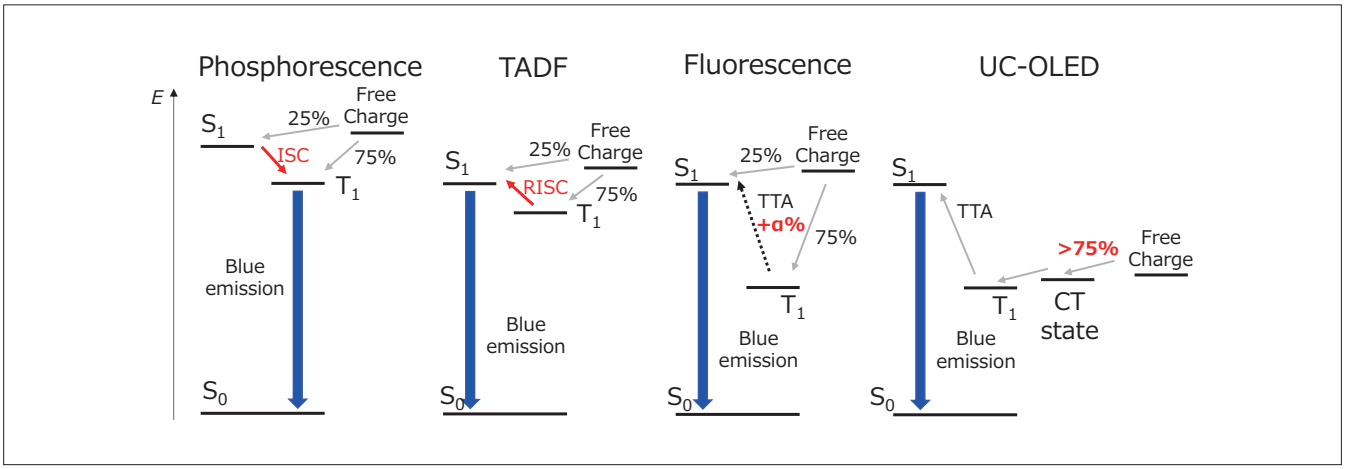

Figure 1. Emission mechanism of phosphorescent, thermally activated delayed fluorescent (TADF), fluorescent, and upconversion (UC) organic light-emitting diodes (OLEDs).

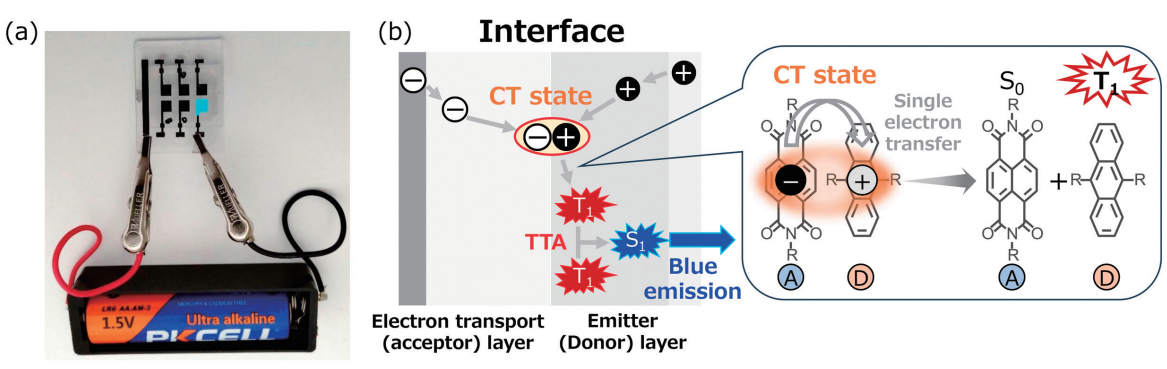

Figure 2. (a) Photograph of blue UC-OLED device operated using only a 1.5 V battery. (b)Transitions of excited states toward blue UC emission.

was proposed over 60 years ago (Figure 3)[9]. According to Marcus theory, the faster the electron transfer rate becomes as the energy difference between the initial and final states increases and approaches the reorganization energy associated with electron transfer (normal region). Conversely, when the energy difference between states is greater than the reorganization energy, the electron transfer rate decreases as the energy difference increases (inverted region). While research on electron transfer processes using Marcus theory has been extensively conducted in fields such as electrode reactions in solution and chemiluminescence, studies at solid-state device interfaces remain limited. This is because it is difficult to accurately evaluate energy levels at interfaces, and since device performance involves many elementary processes, it is challenging to isolate and discuss the efficiency of only the elementary processes related to electron transfer.

3. Fabrication and Evaluation of UC-OLED Devices

Figure 4a shows the structures and energy levels of the highest occupied molecular orbital (HOMO) and lowest unoccupied molecular orbital (LUMO) for the anthracene derivative donor molecule and the naphthalene diimide derivative acceptor molecule used in this study. The donor's HOMO and the acceptor's LUMO were evaluated

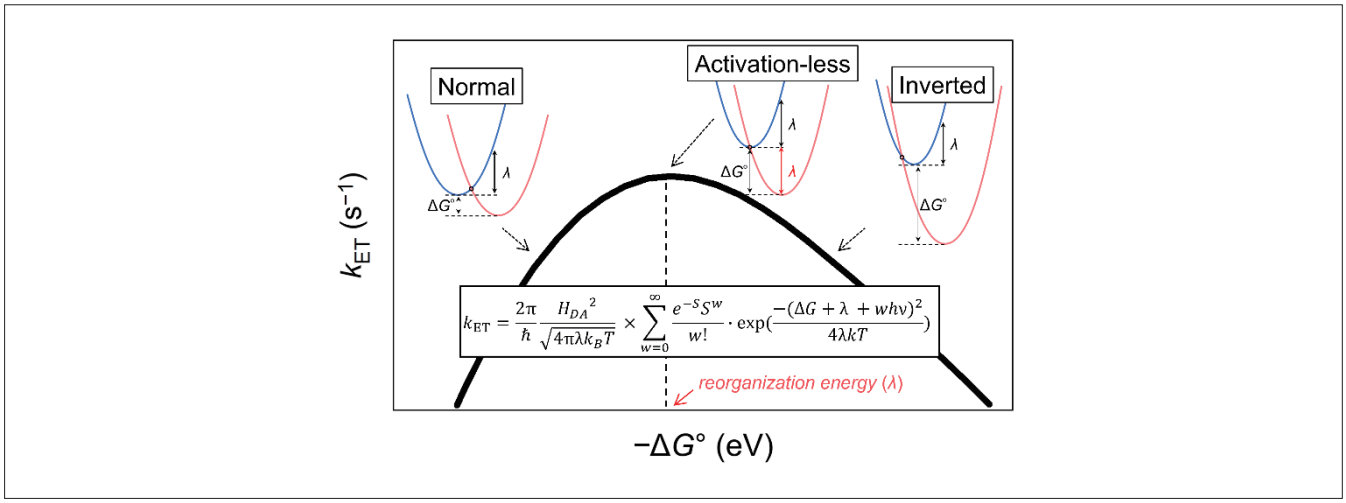

Figure 3. Illustration and equation of the semi-classical Marcus theory. Reproduced from reference 8.

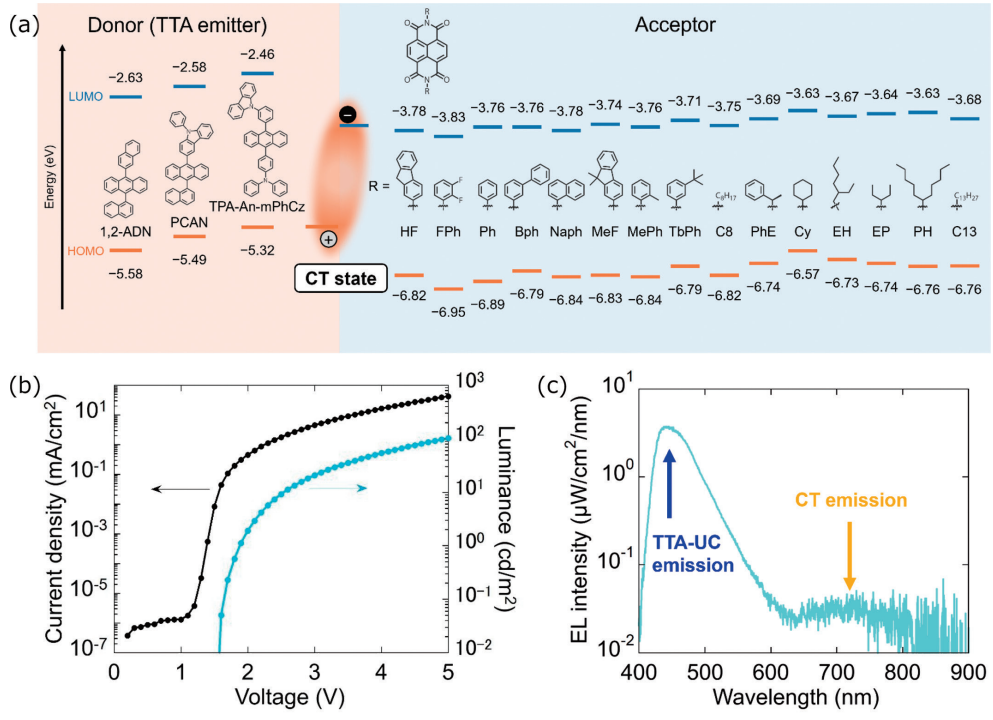

Figure 4. (a) Chemical structures and energy levels of the materials used in this study. (b) *J*-*V* and *L*-*V* curves and (c) EL spectrum of a typical blue UC-OLED device. Reproduced from reference 8.

by cyclic voltammetry, while the donor's LUMO and the acceptor's HOMO were calculated using the optical bandgap values derived from the light absorption edges. Three types of anthracene derivatives—1,2-ADN, PCAN, and TPA-An-mPhCz—were used as donor and TTA emitter molecules. A characteristic of these molecules is that the HOMO level gradually changes depending on the number of electron-donating carbazoles or triphenylamines contained within the molecule. For the acceptor molecules, naphthalene imide derivatives, 15 types of molecules with different side-chain structures attached to the nitrogen atom of the imide group were used. The energy levels can be varied based on the electron-withdrawing or electron-donating properties of the side chains, and the interactions at the D/A interface can also be varied due to differences in steric hindrance caused by the side-chain structures. Since the energy of the CT state generated at the D/A interface is primarily determined by the donor's HOMO and the acceptor's LUMO levels, using these 45 combinations allows for a nearly continuous variation in the CT state energy, thereby clarifying the influence of the energy difference between the CT state and the T_1 level of the anthracene derivative on the electron transfer process. The UC-OLED devices were fabricated using vacuum deposition, with layers stacked in the following order: ITO/MoO_3 (hole injection layer)/anthracene derivative/naphthalene diimide derivative/Py-hpp2 (electron injection layer)/Al. The OLED devices were evaluated based on current-voltage-luminance measurements and emission spectra. Figure 4b shows a typical current-voltage-luminance curve for the UC-OLED, and Figure 4c shows the emission spectrum. First, since the blue emission of the UC-OLED proceeds via the TTA-UC process, it starts at a voltage of approximately 1.5 V, which corresponds to about half the bandgap of the anthracene derivative. Furthermore, examining the emission spectrum reveals blue TTA-UC emission around 450 nm, while CT emission from the D/A interface appears in the low-energy region around 700 nm, which is significantly distant in wavelength.

4. Evaluation of Energy Levels and Effect for Single-Electron Transfer Process

To evaluate the single-electron transfer process from the CT state to the T_1, we first measured the T_1 level in thin films of anthracene derivatives. To optically excite the T_1 of the anthracene derivatives, we performed phosphorescence measurements using thin films of anthracene derivatives doped with PtOEP as a triplet sensitizer. Phosphorescence measurements were performed using a spectrofluorometer (FP-8650). The thin-film samples were cooled to 77 K (−196°C) using a liquid nitrogen cooling unit (PMU-130), and measurements were conducted in phosphorescence mode. Figure 5a shows the phosphorescence spectra of three PtOEP-doped anthracene derivative films and a pristine PtOEP film. Comparison with the spectrum of the pristine PtOEP identified the peak near 700 nm as emission from the T_1 level of the anthracene derivatives. Furthermore, since the device operates at room temperature, phosphorescence measurements were performed while varying the temperature using a cryostat to obtain information on the T_1 level at room temperature. The T_1 levels calculated from the peak wavelengths were plotted against temperature, and the T_1 levels at room temperature, obtained by extrapolation to 300 K, were found to be nearly identical at 1.65 eV for the three anthracene derivatives (Figure 5b).

Combining this with the CT state energy calculated from the CT emission peak of the UC-OLED allows us to determine the energy difference between the CT state and T_1 for each device. Based on the emission mechanism shown in Figure 2b, the emission efficiency of the UC-OLED is represented by the product of the CT state generation efficiency, the single-electron transfer efficiency from the CT state to T_1, the TTA efficiency, and the fluorescence quantum yield (PLQY) of the anthracene derivative. Since the CT state generation efficiency is 75% based on the spin-statistics rule—primarily due to the use of triplet CT—and assuming that the TTA efficiency does

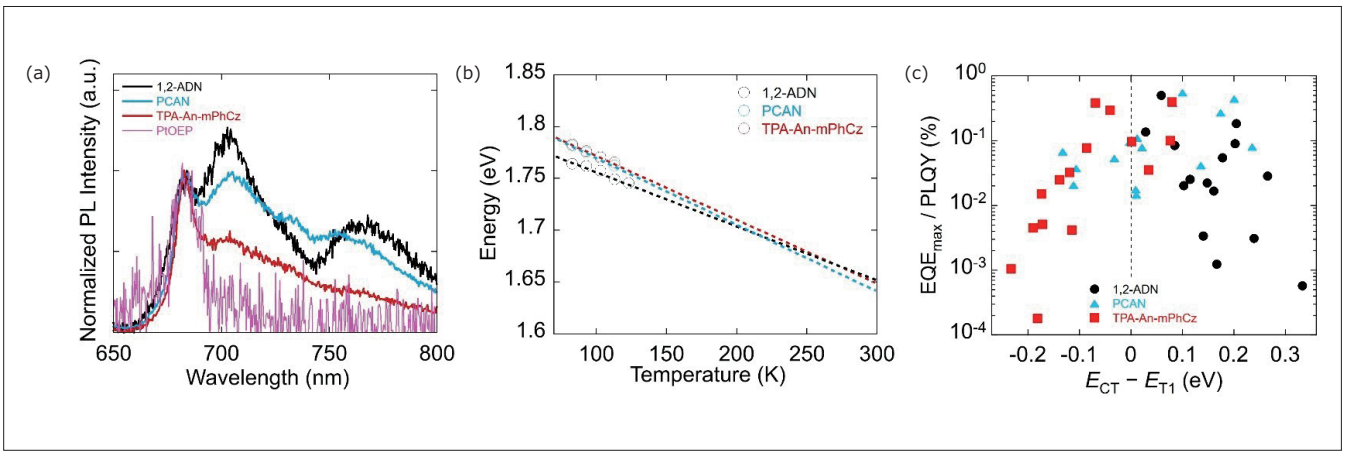

Figure 5. (a) Phosphorescence spectra of the PtOEP-doped 1,2-ADN, PCAN, TPA-An-mPhCz, and PtOEP neat film at an excitation wavelength of 550 nm at 77 K. e) Temperature-dependentce of peak energies of phosphoresce of the PtOEP-doped 1,2-ADN, PCAN, and TPA-An-mPhCz (red). f) Correlation between $E_{CT} - E_{T,}$ and EQE_{max} divided by the PLQY of each donor (TTA emitter). Reproduced from reference 8.

not vary among the anthracene molecules, dividing the UC-OLED's EL efficiency by the PLQY of the anthracene derivative allows us to discuss the single-electron transfer efficiency from the CT state to T_1 across the devices. Therefore, the PLQY of thin-film samples of anthracene derivatives on quartz substrates was measured using a spectrofluorometer (FP-8650) connected to a 120 mm ϕ integrating sphere unit (ILF-135). As a result, the fluorescence quantum yields of 1,2-ADN, PCAN, and TPA-An-mPhCz were found to be 37%, 62%, and 76%, respectively. Using these data, we plotted the values for 45 types of devices with the energy difference between the CT state and T_1 ($E_{CT} - E_{T1}$) on the horizontal axis and the maximum external quantum efficiency (EQE_{max}) of the UC-OLED divided by PLQY on the vertical axis. As shown in Figure 5c, although there is some variation, we found that the plot follows an inverse parabolic shape, as explained by Marcus theory.

In the semi-classical Marcus theory shown in Figure 3, the electron coupling (H_{DA}) in the pre-exponential term, in addition to the energy difference, influences the electron transfer rate. Therefore, we hypothesized that the variation in the plot shown in Figure 5c was due to differences in the interactions at the D/A interface, and we measured the absorption intensity of the CT state to evaluate these interfacial interactions. Since CT state absorption is weak due to intermolecular transitions and is difficult to observe using conventional optical absorption measurements, we observed it by sensitively measuring the photocurrent response of the UC-OLED device. Since this measurement is equivalent to sensitive measurement of the external quantum efficiency (EQE) or incident photon-to-current efficiency (IPCE) in solar cells, it was performed using a high-sensitivity spectroscopic measurement system (HQE-25DK) manufactured by Bunkoukeiki. This measurement system eliminates stray light using a double monochromator and employs a low-noise Keithley 6430 sub-femtampere remote source meter, enabling the measurement of highly sensitive photocurrent responses corresponding to interfacial absorption. Figure 6a shows the IPCE spectra of UC-OLEDs with 1,2-ADN and various naphthalene derivative molecules. A shoulder corresponding to clear CT state absorption was observed in the low-energy region, and the CT absorption intensity was calculated by fitting this with a Gaussian function. Assuming this CT absorption intensity corresponds to the electron coupling at the D/A interface, Figure 6b shows a plot of the values obtained by dividing the vertical axis of Figure 5c by the CT absorption intensity. The variation was smaller than in Figure 5c, and it was found that the data could be successfully fitted using the semi-classical Marcus equation shown by the dotted line. Figure 6b covers a wide range from the normal region to the inverted region, revealing that the electron transfer efficiency between states is maximized when the energy difference between the CT state and T_1 is near zero. From the fitting using the semi-classical Marcus theory, the reorganization energy λ was calculated to be 0.08 eV; thus, it was found that keeping the energy difference between states at 0.1 eV or less is effective for promoting this electron transfer process. In OLEDs, the energy difference between excited states leading to light emission serves as both the driving force for promoting transitions between states and a source of energy loss required to generate light. The discovery that excited-state transitions can be promoted with a very small driving force indicates that the interfacial electron transfer process leading to TTA-UC emission in UC-OLEDs has achieved an ideal situation for low energy loss—that is, for operation at low voltage.

5. Summary and Outlook

In summary, we fabricated and evaluated UC-OLEDs in which the energy of the CT state was continuously varied using 45 different combinations of donor and acceptor molecules. We obtained Marcus plots of the single-electron transfer process associated with the transition from the CT state to T_1, spanning from the normal region to the inverted region. Analysis revealed that in a very

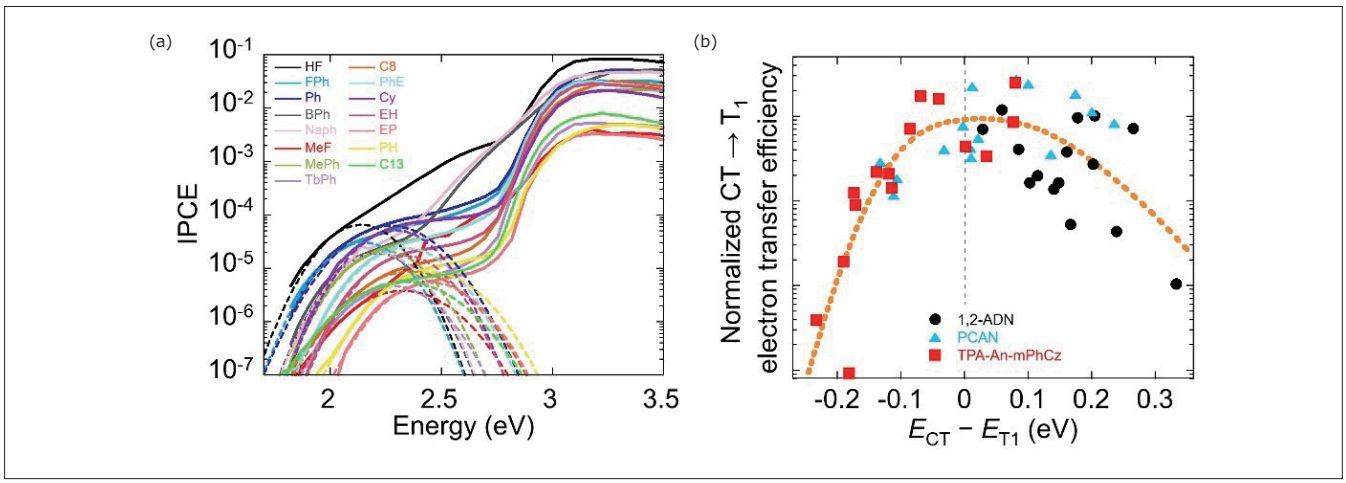

Figure 6. (a) IPCE spectra and their fitting curves of the 1,2-ADN/acceptor-based devices. (b) Correlation between $E_{CT} - E_{T_1}$ and the normalized electron transfer efficiency from the CT state to T_1 and fitted curve using the semi-classical Marcus theory. Reproduced from reference 8.

small energy gap of 0.1 eV or less between the CT state and T_1, the single-electron transfer process is accelerated, enabling efficient TTA-UC emission[8]. Since the energy difference between excited states leading to luminescence results in energy loss—that is, voltage lloss—the ability to promote electron transfer with the smallest possible energy gap indicates that an ideal condition for low-voltage operation of UC-OLEDs has been achieved.

Furthermore, we continue to advance UC-OLED research. By developing not only donor and acceptor molecules but also the fluorescent dopant that finally emits light, we have succeeded in achieving deep blue emission below 450 nm with a narrow half-width of approximately 20 nm at low voltage, suitable for display applications[10], as well as low-voltage white emission suitable for lighting applications[11]. Recently, we have also reported UC-OLEDs based on a new material system that can emit light in the ultraviolet to violet region at voltages below 2 V by using novel TTA emitters[12]. We believe that UC-OLEDs are an interesting subject for photochemical research, not only in terms of OLED device development aimed at low-voltage emission and, consequently, low energy conservation, but also because they allow for the selective observation of TTA-UC and interfacial emission through current excitation.

Acknowledgements

This research was supported in part by JSPS KAKENHI, Grants-in-Aid for Scientific Research (21H05411, 22K14592), JST PRESTO (JPMJPR2101), JST A-STEP (JPMJTR23R8) and The Morino Foundation for Molecular Science. The author would like to thank M. Morimoto and S. Naka at Toyama University, K. Fujimoto and M. Takahashi at Shizuoka University, M. Hiramoto at Institute for Molecular Science, K. Nakayama at The University of Osaka, N. Aizawa at Hokkaido University, and Y. Majima, H. Iwasaki, Q. Shui, Y. Yang, D. Nakahigashi at Institute of Science Tokyo for their collaboration to the research.

● References

1) M. A. Baldo, D. F. O'Brien, Y. You, A. Shoustikov, S. Sibley, M. E. Thompson, S. R. Forrest, *Nature* **395**, 151 (1998).
2) H. Uoyama, K. Goushi, K. Shizu, H. Nomura, C. Adachi, *Nature*, **492**, 234 (2012)
3) J. Hu, Y. Pu, F. Satoh, S. Kawata, H. Katagiri, H. Sasabe, J. Kido, *Adv. Funct. Mater.*, **24**, 2064 (2014)
4) D. Wang, C. Cheng, T. Tsuboi, Q. Zhang, *CCS Chem.* **2**, 1278 (2020).
5) S. Izawa, M. Hiramoto, *Nat. Photon.*, **15**, 895 (2021)
6) S. Izawa, M. Morimoto, S. Naka, M. Hiramoto, *Adv. Opt. Mater.*, **10**, 2101710 (2022)
7) S. Izawa, M. Morimoto, K. Fujimoto, K. Banno, Y. Majima, M. Takahashi, S. Naka, M. Hiramoto, *Nat. Commun.*, **14**, 5494 (2023)
8) H. Iwasaki, K. Fujimoto, K. Banno, Q. Shui, Y. Majima, M. Takahashi, S. Izawa, *Angew. Chem. Int. Ed.*, **63**, e202407368 (2024)
9) R. A. Marcus, *Angew. Chem. Int.* **32**, 1111 (1993)
10) Q. Shui, H. Iwasaki, D. Nakahigashi, Y. Majima, S. Izawa, *Adv. Opt. Mater.*, **13,** e01576 (2025)
11) Y. Yiyan, Q. Shui, H. Iwasaki, D. Nakahigashi, Y. Majima, K. Nakayama, N. Aizawa, S. Izawa, *J. Mater. Chem. C*, **13**, 16963–16968 (2025)
12) 岩崎，真島，伊澤：第73回応用物理学会春季学術講演会，18a-M_B104-6（2026）

いざわ　せいいちろう
東京科学大学　総合研究院　フロンティア材料研究所　准教授／博士（工学）

筆者紹介　2015年　東京大学大学院応用化学専攻博士課程修了　2015–2016年　日本学術振興会特別研究員PD、理化学研究所訪問研究員、カリフォルニア大学サンタバーバラ校訪問研究員、2016–2022年　分子科学研究所助教、2021–2025年　JSTさきがけ研究者（兼任）、2023–2024年　東京工業大学　科学技術創成研究院　フロンティア材料研究所　准教授、2024年–東京科学大学　総合研究院　フロンティア材料研究所　准教授　《現在の研究テーマ》有機半導体界面を使った光機能・デバイスの開拓